WARSAW UNIVERSITY OF TECHNOLOGY Index 351733
FACULTY OF CIVIL ENGINEERING
COMMITTEE FOR CIVIL AND WATER ENGINEERING
POLISH ACADEMY OF SCIENCES ISSN 1230-2945

DOI: 10.24425/ace.2020.131796

ARCHIVES OF CIVIL ENGINEERING

Vol. LXVI ISSUE 2 2020



# FIRE RESISTANCE ASSESSMENT OF THE LONG-SPAN STEEL TRUSS GIRDER

**P. WOŹNICZKA[1]**

The performance-based analysis of the large-space steel sports hall is presented. Load-bearing structure of the hall consists of spatial long-span truss girders that are made of modern square hollow sections. Both fire development analysis and mechanical response analysis are discussed in detail. Fire Dynamics Simulator and Safir programs are used. Main focus is put on the factors that could affect the final fire resistance of the structure. Uniform and non-uniform heating, different boundary conditions and local imperfections are taken into account. Structures with and without fireproof insulation are considered. Values of the critical temperature, failure modes and fire resistance estimated for various cases are presented. Computer simulations were carried out both for fire growth and decay phase. As a result it is clearly shown that some reductions of the required fireproof insulation are possible. Moreover, the structure without complete traditional fireproof insulation is able to survive not only the direct fire exposure but also the cooling phase.

*Keywords*: fire resistance, large-space hall, fire, performance-based analysis

[1] PhD. Eng., Cracow University of Technology, Faculty of Civil Engineering, Warszawska 24, 31-155 Cracow, Poland, e-mail: pwozniczka@pk.edu.pl

# 1. INTRODUCTION

Current standard EN 1993-1-2 [2] provides a wide range of advanced analysis methods that could be used in order to evaluate the fire resistance of steel members or even whole structures. An advanced approach must consist of both fire development analysis and modelling of the mechanical response of the structure. Application of the previously mentioned methodology is mainly addressed in reference to more complex fire zones rather than for typical compartments. Profits from using it, such as possible reduction of expensive fireproof insulation and better insight into the behaviour of the structure, can be especially significant for commonly found large-space steel halls. Conversely, advanced analysis methods are time-consuming and require appropriate knowledge in terms of fire and civil engineering. Moreover, some crucial factors such as impact of local imperfections are still not fully recognised. In the result existing examples of such analysis are at the moment limited to just a few cases that have been recently described in [8], [12] and [13]. In this situation some further research is required.

In the following paper the performance based analysis for the large-space sports steel hall is presented. According to the classification that is given in [7] the hall can be considered as the building with both a very large floor area and significant height. Special attention is focused on the fire behaviour of the spatial long-span truss girder that is subjected to uniform and non-uniform heating. Moreover, some remarks regarding the impact of imperfections and boundary conditions are discussed. Values of the critical temperature, possible failure modes, changes in the level of internal forces and deformations of the structure are presented. The analysis is carried out not only for the fire growth phase but also for the decay phase.

# 2. DESCRIPTION OF THE STEEL HALL

Described sports hall was 70m long and 60m wide. The height of the main compartment was 16.5m. The cross-section through the hall is presented in Fig.1a. External load-bearing walls, columns and stands were made of reinforced concrete. The roof structure consisted of 9 steel spatial truss girders that were set in 6m spacing. Each spatial truss had two top chords and one bottom chord. Top chords were made of square hollow sections (SHS) 200x10, while the bottom chord was formed from SHS 250x10. For the internal members of the truss girder SHS 80x8 were used. The diagonals between top chords were formed from SHS 60x5. All sections were made of S355 steel grade.

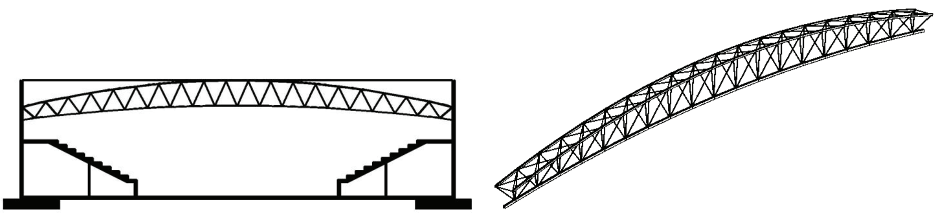

a) b)

Fig. 1. a) Cross-section through the considered steel hall, b) the view of the spatial truss girder.

The view of the truss girder is presented in Fig. 1b. The roof was made of trapezoidal sheeting spanning between the trusses. The main structure did not require any additional bracings and each truss could be analysed separately. At the ends of the truss pinned supports were designed. However horizontal displacements (limited to 5cm) were allowed on the one side in order to provide some necessary heat compensation. For the accidental combination of actions uniformly distributed load on each top chord was 3.0kN/m. The reduction factor $\eta_{fi}$ [2] was rather typical for steel halls and it was equal to 0.52.

## 3. FIRE DEVELOPMENT ANALYSIS

Characteristic value of fire load density was 300MJ/m2 for the stands and 285MJ/m2 for the floor in the middle of the hall. Scenario of localised fire was taken into consideration. Maximum fire power was Q=10MW and it was estimated according to the data given in [3]. This value was appropriate for sports halls without any fire devices such as e.g. sprinklers. Due to the results of own computer simulations possibility of further fire spread and flashover was taken into account. It was assumed that most of the equipment was made of plastic, so the ignition temperature for the storaged goods was set up for 350°C. Rate of heat release was taken conservatively as 500kW/m2. As a result the initial fire area was 4.5m by 4.5m. Fire growth was described according to t-square formula. Fire growth rate was taken such as for the fast fire according to [1]. Computer simulations were performed using the Fire Dynamics Simulations program [11]. The whole computational volume of the building was divided into 0.5x0.5x0.5m finished elements. However, near the fire source finer mesh (0.25x0.25x0.25m) was applied. $D/\delta^*$ ratio calculated according to [11] was in this situation equal to 9.63.

Three initial fire locations were taken into account. First location (L1) was just near the external wall of the hall, at the top of the stand at the height of 8m above the floor level. The second place which was considered was in the distance of 9m from the first one at the height of 6m above the floor (L2, presented in Fig. 2). Finally the last scenario involved localised fire that was set at the floor level in the middle of the sports hall (marked as L3). For each initial fire location simulations were performed for at least two hours of fire development. In none of the considered cases ignition of the storaged goods occurred. Thus, the fire remained at the stage of localised fire.

Comparison of the estimated values of the temperature at the level of lower chords for L1 and L2 cases is presented in Fig 3. One can notice that the highest values of the temperature for L1 case were obtained. Level of 800°C that was achieved could be a serious threat for the unprotected steel structure. For L2 position maximum value of the temperature was close to 300°C. Similar maximum temperature was obtained for L3 situation. Differences in the results for mentioned fire scenarios were easy to justify. First of all the distance between the fire source and the truss is the shortest for L1 case. This effect is additionally increased by the parabolic shape of the arch truss girder. It should be also noticed that due to the low fire load density the fire expired just after around 1500s. Thus, the fire exposure of the truss was not especially long-lasting.

It was decided that L1 case is the most appropriate fire scenario and it was used during the further mechanical analysis. In order to apply possibly accurate values of the temperature for non-uniform heating of the structure numerous thermocouples were arranged along the span of the truss. At least one thermocouple was assigned to each joint of the truss and their location is presented in Fig. 4. Moreover, in Fig. 4 the fire curves that were obtained for selected thermocouples are given. One can see that there is a significant difference between values of the temperature for lower and upper chord. This could be explained by the height of the truss and low initial power of the considered localised fire. Also the reason for the low and nearly constant temperature that was estimated for thermocouples localised in some distance from the fire source was not sufficient fire power (e.g. fire curve related to "G" thermocouple in Fig. 4)

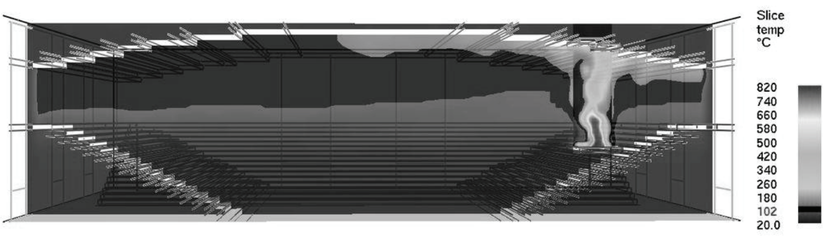


Fig. 2. Temperature distribution in the sports hall in the case of localised fire.

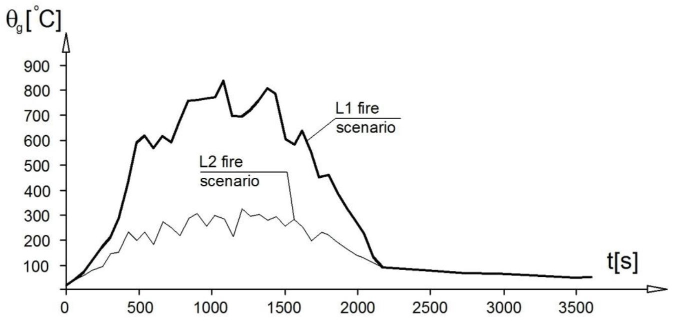


Fig. 3. Comparison of temperature measured at the level of the lower chord. Fire scenarios L1 and L2.

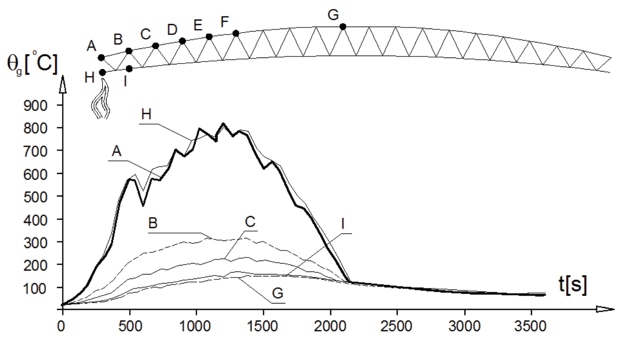


Fig. 4. Fire curves received for thermocouples arranged along the span of the truss (case L1). Results for D,E, and F are not presented in order to provide clearness of the figure. D,E,F fire curves are contained between C and G.

## 4. STRUCTURAL ANALYSIS

For the considered truss girder mechanical response analysis using Safir program [5] was performed. Prismatic Bernoulli type beam elements with some additional warping freedom degree at the end nodes were used. Each member was divided into 20 cm long finished elements. Dynamic approach as the most suitable for fire design was applied. Comeback parameter was equal to 1E-4 and precision was set as 1E-5. For Class 1 cross-sections the STEELEC3EN material was used. For the remaining classes it was decided to use the advanced STEELSL material [4] which allowed to take into account local buckling phenomenon and limited rotation capacity. For comparison reasons the girder was uniformly heated according to nominal fire curve. Then it was calculated again using non-uniform temperature distribution. In this case, for simplicity reasons, it was necessary to divide truss into some separate parts which were heated according to selected individual fire curves presented previously in Fig.4. Division of the truss with assigned fire curves (A,B,C etc. according to Fig.4) is presented in Fig 5.

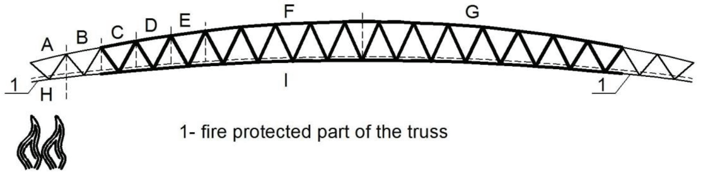


Fig. 5. Fire curves assigned to different parts of the truss.

Different boundary conditions were taken into account, i.e. horizontal displacements were allowed or restricted. For some cases local imperfections for compressed members were added to the structural model. All prepared computer models are listed in Table 1. In the case of the structure that was able to survive the initial phase of the fire it was also necessary to continue the simulations during the cooling phase. In the current standard [2] it was not explained how to estimate the permanent reduction of steel properties after the fire exposure. In this situation equations given in [10] were adopted. Eq. (4.1), (4.2) and (4.3) should be used to calculate yield stress reduction factor while Eq. (4.4) and (4.5) should be used to calculate Young's modulus reduction factor. Further details concerning the permanent reduction of the mechanical properties for steel exposed to elevated values of temperature can be found in [9].

Table 1. Computer models of the considered sports hall

| Model | Fireproof insulation | Horizontal displacement of the support | Fire model | Local imperfections |
|---|---|---|---|---|
| SD3 | no | allowed | nominal fire curve | no |
| SD3-ih | no | allowed | nominal fire curve | yes |
| SD3b | no | limited to 5cm | nominal fire curve | no |
| SD3+PN | no | allowed | natural fire | no |
| SD3b+PN | no | limited to 5cm | natural fire | no |
| SD3+PN+izo | yes | allowed | natural fire | no |
| SD3b+PN+izo | yes | limited to 5cm | natural fire | no |
| SD3-ih+PN+izo | yes | allowed | natural fire | yes |

(4.1) $$k_{y.permanent} = 1 \text{ for } \Theta_s \leq 600°C$$

(4.2) $$k_{y.permanent} = 1.504 - \Theta_s / 1200 \text{ for } 600°C < \Theta_s < 900°C$$

(4.3) $$k_{y.permanent} = 0.748 \text{ for } \Theta_s \geq 900°C$$

(4.4) $$k_{E.permanent} = 1 \text{ for } \Theta_s \leq 600°C$$

(4.5) $$k_{E.permanent} = 1.431 - \Theta_s / 1400 \text{ for } \Theta_s > 600°C$$

where:

$\Theta_s$ – temperature of steel

# 5. RESULTS OF THE PERFORMANCE-BASED ANALYSIS

Main results of the analysis are presented in Table 2. For the cases that were calculated without taking into account fire protection the most important factor that affected fire resistance were boundary conditions. For example fire resistance estimated for SD3b case is almost two times lower than for SD3 case. This result was expected because restricted displacements were generating higher internal forces. However this was not the case for simulations based on natural fire model. In SD3+PN model calculations were stopped after 1138s while for SD3b+PN it happened after 1401s. This dissimilarity

Table 2. Results of the advanced structural analysis

| Model | Fire resistance [s] | Failure mode | Maximum deflection [cm] | Critical temperature [°C] |
|---|---|---|---|---|
| SD3 | 865 | Buckling of the SHS 80x8 diagonals (near the support) | -61 | 610 |
| SD3-ih | 825 | Buckling of the SHS 80x8 diagonals (near the support) | -34 | 585 |
| SD3b | 380 | Buckling of the SHS 80x8 diagonals (near the support) | +30 | 300 |
| SD3+PN | 1138 | Buckling of the SHS 80x8 diagonals (near the support) | -40 | 652 |
| SD3b+PN | 1401 | Buckling of the top chord (near the support) | -9 | 695 |
| SD3+PN+izo | >7200s | --- | -12 | --- |
| SD3b+PN+izo | >7200s | --- | -12 | --- |
| SD3-ih+PN+izo | >7200s | --- | -12 | --- |

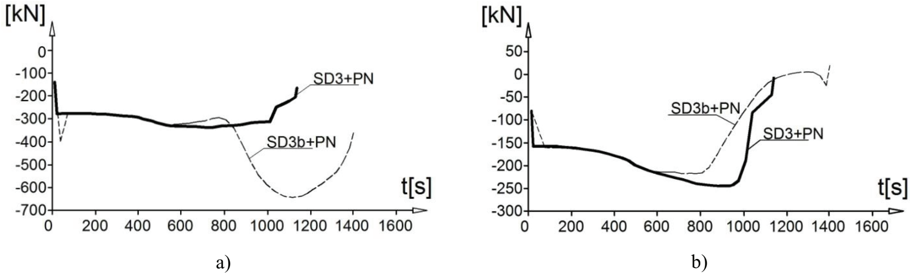


Fig. 6. Comparison between SD3+PN and SD3b+PN. Axial force: a) for the top chord, b) for the diagonal.

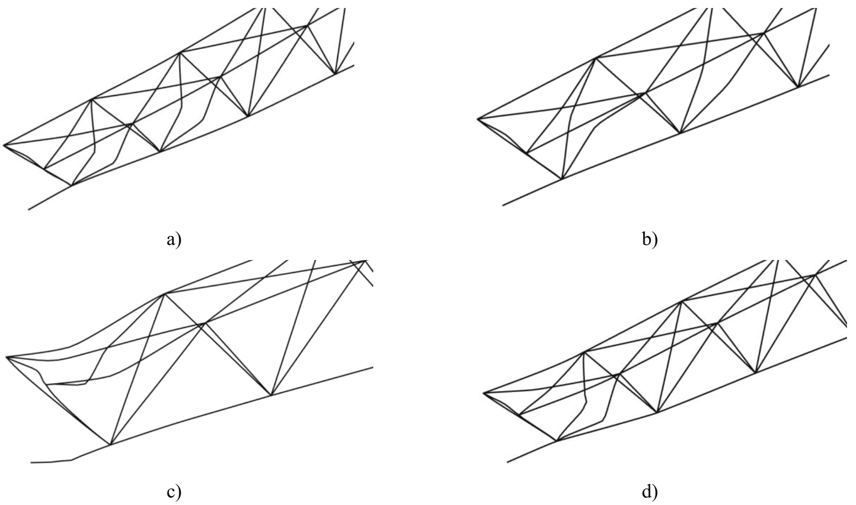


Fig. 7. Failure modes: a) SD3, b) SD3-ih, c) SD3b+PN, d) SD3+PN.

could be explained by the behaviour of the structure. For SD3b+PN case, when all available displacements were used, the main part of arising internal forces was carried by the top chords. In this situation they could be considered as arches. Simultaneously the forces in lower chord and diagonals decreased. In the result the failure of the diagonals was not observed. For SD3+PN there was no possibility for such forces redistribution so the diagonals remained the weakest point of the truss. The same mechanism was not able to develop for uniformly heated truss (SD3b) and this was due to significantly higher thermal elongations and in the result higher internal forces. For SD3b maximum value of the axial compression force was 1600kN (t=350s) while for SD3b+PN it was just 650kN. In Fig. 6 comparison of the internal forces for top chord and for the diagonal is presented. For all performed simulations the failure modes were similar and they were related to the buckling of the diagonals near the support. The only exception was SD3b+PN model where arch behaviour of top chords was observed. Selected failure modes are given in Fig. 7.

It should be also mentioned that predicted fire resistance wasn't strongly affected by applied local imperfections. For example for SD3 and SD3-ih cases reduction of the fire resistance was equal to 40s which is only around 5% of the total fire resistance. Also the same failure modes were observed for both cases. One can also see that obtained values of the critical temperature did not depend on the way of structural modelling. For nearly all cases (except case SD3b) they contained in the range from 585°C to 695°C. Slightly higher values were noticed for non-uniformly heated models.

However all previously described simulations could not be treated as a success. Despite taking into account advanced fire scenarios and different boundary conditions it was not possible to satisfy the R30 criterion (load bearing function maintained for at least 30 minutes of fire exposure). In such situation it was decided to apply fireproof insulation. However unlike for the traditional approach it was not necessary to provide it for the whole girder. Thus, only members that were at a distance of 7m from supports became protected. It was assumed that fireproof insulation is made of mineral fibre spray. Properties of the spray (λ=0.12W/mK, cp=1200J/kgK, ρ=300kg/m3) were taken from [6]. Three further cases of computer simulations (Table 2) were prepared (SD3+PN+izo, SD3b+PN+izo and SD3-ih+PN+izo). For all of them structure was able to survive not only the initial phase of fire development but also the cooling phase. The simulations were carried out for two hours since the fire ignition. However it was noticed that after this time the temperature of both protected and unprotected steel members was still slightly increased (40°C and 90°C respectively). Therefore to avoid unnecessary time-consuming calculations resulting from thermal capacity of the whole building it was decided to reduce immediately the value of the temperature for all members to 20°C after 7500s. Fig. 8 presents the variation of the axial force and deflections for partially fire protected girder. One can notice that after fire exposure both internal forces and displacements returned to the initial level.

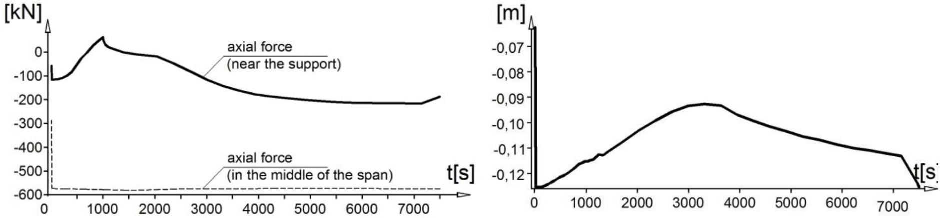


a) b)

Fig. 8. Case SD3-ih+PN+izo: a) axial force (top chord), b) vertical displacements in the middle of the span.

# 6. CONCLUSIONS

The complete case of performance-based analysis carried out for a large-space steel hall was discussed. Different fire scenarios were analysed in order to estimate non-uniform fire temperature distribution across the hall. Factors that influence the fire resistance of load-bearing structure were presented. Performed research indicated that application of both advanced fire development analysis and mechanical response analysis allowed to reduce significantly required fireproof insulation. Furthermore, structure was able to survive not only the direct fire exposure but also the cooling phase. Impact of the boundary conditions and assigned fire curves seemed to be crucial for carried out computer simulations. Explanation of the influence of the local imperfections require further extended analysis.

# REFERENCES


1. EN 1991-1-2 Eurocode 1: Actions on structures exposed to fire. CEN, Brussels, Belgium, 2005.
2. EN 1993-1-2 Eurocode 3: Design of steel structures. Part 1-2: General rules - Structural fire design, CEN, Brussels, Belgium, 2005.
3. S-G. Fan, G-P. Shu, G-J. She, J.Y.R. Liew, "Computational method and numerical simulation of temperature field for large-space steel structures in fire", Advanced Steel Construction 10(2): 151-178, 2014
4. J-M. Franssen, B. Cowez, T. Gernay, "Effective stress method to be used in beam finite elements to take local instabilities into account", Fire Safety Science, Proceedings of the 11th IAFSS Symposium, Christchurch, New Zealand: 544-557, 2014.
5. J-M.Franssen, T. Gernay, "Modelling structures in fire with SAFIR: Theoretical background and capabilities", Journal of Structural fire Engineering 8(3): 300-323, 2017.
6. J-M. Franssen , P. Vila Real, "Fire Design of Steel Structures". Second ed.: ECCS, Ernst & Sohn, 2015.
7. G. Li, P. Wang, "Advanced analysis and Design for Fire Safety of Steel Structures". Heidelberg: Springer, 2013.
8. L. Lu, G. Yuan, Z. Huang, Q. Shu, Q. Li, "Performance-based analysis of large steel truss roof structure in fire", Fire Safety Journal 93: 21-38, 2017.
9. M. Maślak, G. Żwirski, "Changes in structural steel microstructures following heating and cooling episodes in fire", BiTP 48(4): 34-52, 2017.
10. C. Maraveas, Z. Fasoulakis, "Post-fire mechanical properties of structural steel", 8th National Steel Structure Conference, Tripoli, Greece.
11. K. McGrattan, S. Hostikka, R. McDermott, J. Floyd, C. Weinschenk, K. Overholt, "Fire Dynamics Simulator User's Guide". Sixth ed.: NIST Special Publication 1019, 2017.
12. L. Pyl, L. Schueremans, W. Dierckx, I. Gieorgieva, "Fire safety analysis of a 3D frame structure based on a full-scale fire test", Thin-Walled Structures 61: 204-212, 2012.
13. G. Zhang, G. Zhu, G. Yuan, Q. Li, "Overall stability analysis of oversized steel-framed building in a fire", Fire and Materials 40: 273-288, 2016

## LIST OF FIGURES AND TABLES:

Fig. 1. a) Cross-section through the considered steel hall, b) the view of the spatial truss girder.

Rys. 1. a) Przekrój poprzeczny przez rozpatrywaną halę, b) widok kratownicy przestrzennej.

Fig. 2. Temperature distribution in the sports hall in the case of localised fire.

Rys. 2. Rozkład temperatury w hali sportowej dla scenariusza pożaru lokalnego.

Fig. 3. Comparison of temperature measured at the level of the lower chord. Fire scenarios L1 and L2.

Rys. 3. Porównanie wartości temperatury na poziomie pasa dolnego. Scenariusze pożarowe L1 i L2.

Fig. 4. Fire curves received for thermocouples arranged along the span of the truss (case L1). Results for D,E, and F are not presented in order to provide clearness of the figure. D,E,F fire curves are contained between C and G.

Rys. 4. Krzywe pożarowe otrzymane dla czujników termicznych rozmieszczonych wzdłuż kratownicy (przypadek L1). Wyniki dla D,E i F nie zostały przedstawione dla zapewnienia przejrzystości wykresu. Krzywe D,E,F zawierają się pomiędzy krzywymi C i G.

Fig. 5. Fire curves assigned to different parts of the truss.

Rys 5. Krzywe temperatury przypisane do poszczególnych fragmentów dźwigara.

Fig. 6. Comparison between SD3+PN and SD3b+PN. Axial force: a) for the top chord, b) for the diagonal.

Rys. 6 Porównanie modeli SD3+PN i SD3b+PN. Siła osiowa: a) w pasie górnym, b) w krzyżulcu.

Fig. 7. Failure modes: a) SD3, b)SD3-ih, c) SD3b+PN, d) SD3+PN.

Rys. 7. Model zniszczenia: a) SD3, b)SD3-ih, c) SD3b+PN, d) SD3+PN.

Fig. 8. Case SD3-ih+PN+izo: a) axial force (top chord), b) vertical displacements in the middle of the span.

Rys. 8. Model SD3-ih+PN+izo: a) siła osiowa (pas górny), b) przemieszczenie pionowe w środku rozpiętości.

Tab. 1. Computer models of the considered sports hall

Tab. 1. Modele komputerowe opracowane dla rozpatrywanej hali sportowej

Tab. 2. Results of the advanced structural analysis

Tab. 2. Wyniki zaawansowanej analizy odpowiedzi mechanicznej konstrukcji

**OCENA ODPORNOŚCI OGNIOWEJ STALOWEJ KRATOWNICY O DUŻEJ ROZPIĘTOŚCI**

*Słowa kluczowe*: odporność ogniowa, hala wielkogabarytowa, pożar, analiza oparta na właściwościach

**PODSUMOWANIE:**

Aktualne normy europejskie EN 1991-1-2 i EN 1993-1-2 dopuszczają do stosowania różnorodne metody oceny odporności ogniowej, które mogą być wykorzystane zarówno w odniesieniu do pojedynczych elementów jak i całych ustrojów nośnych. Podejście obliczeniowe bazujące na właściwościach danej strefy pożarowej (tzw. performance-based approach) powinno uwzględniać zarówno analizę rozwoju pożaru jak i odpowiedzi mechanicznej konstrukcji. Wykorzystanie tego typu metody może być szczególnie istotne w przypadku obiektów o stosunkowo dużych kubaturach stref pożarowych, takich jak na przykład wielkogabarytowe hale o konstrukcji stalowej. Możliwy jest wówczas nie tylko lepszy wgląd w zachowanie się konstrukcji w warunkach pożaru ale istnieje także możliwość dostosowania izolacji ogniochronnej do rzeczywistego zapotrzebowania. Jednocześnie przeprowadzenie kompletnych symulacji typu "performance-based" jest niezwykle czasochłonne oraz wymaga połączenia wiedzy z zakresu inżynierii pożarowej oraz inżynierii lądowej. Dodatkowo wpływ niektórych czynników (takich jak przykładowo lokalne imperfekcje łukowe) na prognozowaną odporność ogniową nie został do tej pory w pełni rozpoznany.

W tej sytuacji w artykule przedstawiono opartą na charakterystyce danej strefy pożarowej analizę odporności ogniowej wielkogabarytowej hali sportowej o konstrukcji stalowej. Rozpatrywana hala charakteryzuje się zarówno znacznymi wymiarami w rzucie (70m x 60m) jak i stosunkowo dużą wysokością (16.5m). Główny ustrój nośny składa się z trójpasowych dźwigarów kratowych o rozpiętości 60m, rozmieszczonych w rozstawie co 6m. Obliczenia rozwoju pożaru wykonano za pomocą programu Fire Dynamics Simulator. Do opracowania analizy odpowiedzi mechanicznej konstrukcji wykorzystano program Safir.

W pierwszym etapie badań przeprowadzono symulacje mające na celu wskazanie najbardziej niekorzystnego scenariusza pożarowego. W przypadku obiektu wielkogabarytowego uwzględniono model pożaru lokalnego rozwijającego się według zależności t-kwadrat. Maksymalną moc pożaru lokalnego określono na Qc=10MW, jednak w opracowanych modelach komputerowych uwzględniono także możliwość zapłonu materiałów wykończeniowych. Wykazano, że najwyższe wartości temperatury zostały osiągnięte w przypadku umieszczenia początkowego źródła ognia bezpośrednio w rejonie podpory dźwigara kratowego. Dla pozostałych scenariuszy pożarowych wartości temperatury na poziomie pasa dolnego kratownicy nie przekroczyły poziomu 300°C.

W drugim etapie badań opracowano modele odpowiedzi mechanicznej konstrukcji. Szczególną uwagę poświęcono zagadnieniom związanym z równomiernym i nierównomiernym ogrzewaniem konstrukcji. W przypadku równomiernego ogrzewania zastosowano krzywą standardową ISO. Konstrukcja ogrzewana nierównomiernie została podzielona na fragmenty, przy czym każdemu z nich przypisano odpowiednią, wyznaczoną uprzednio za pomocą modelu obliczeniowej mechaniki płynów, krzywą pożarową. W obliczeniach uwzględniono również wpływ lokalnych imperfekcji łukowych oraz przyjętych warunków brzegowych. Symulacje komputerowe prowadzono zarówno dla fazy wzrostu pożaru jak i dla fazy stygnięcia. W modelu komputerowym wprowadzono trwałą redukcję właściwości mechanicznych stali po przekroczeniu wartości temperatury 600°C.

W wyniku przeprowadzonych badań określono wartości temperatury krytycznej, wskazano potencjalne modele zniszczenia oraz przeanalizowano deformacje i zmiany wartości sił wewnętrznych kratownicy. W zależności od przyjętych danych wejściowych szacowana odporność ogniowa wahała się między 380s a 1401s. Wymaganą odporność

ogniową R30 udało się uzyskać tylko dla dźwigarów dla których wprowadzono izolację ogniochronną fragmentów konstrukcji. Przeprowadzone symulacje komputerowe wskazują, że dzięki zastosowaniu zaawansowanej analizy obliczeniowej istnieje możliwość ograniczenia zakresu stosowania izolacji ogniochronnej. Stwierdzono również, że przy ograniczonych zabezpieczeniach ogniochronnych analizowana konstrukcja jest w stanie przetrwać zarówno fazę wzrostu jak i fazę stygnięcia pożaru. Wskazano, że przyjęte warunki brzegowe i zastosowany sposób ogrzewania były decydujące dla oszacowanej odporności ogniowej konstrukcji. Jednocześnie w większości przypadków wartości temperatury krytycznej zawierały się w przedziale 585°C do 695°C. Również potencjalne formy zniszczenia zaobserwowane dla poszczególnych modeli były do siebie zbliżone.

Received 07.09.2019, Revised 02.04.2020